**Figure 6.1.** *Square-wave bursting. Note that the active phase of repetitive firing is at membrane potentials more polarized than during the silent phase. Moreover, the frequency of spiking slows down at the end of the active phase.*

6.2 Square-wave Bursters

Perhaps the best studied form of bursting is so-called *square-wave bursting*. This class of bursting was first considered in models for electrical activity in pancreatic-beta cells; these play an important role in the release of insulin. Another example of square-wave bursters is respiratory generating neurons within the Pre-Botzinger complex.

An example of a square-wave burster is shown in Figure 6.1. Note that the active phase of repetitive firing occurs at membrane potentials considerably more polarized than during the silent phase. Another feature of square-wave bursting is that the frequency of spiking slows down during the active phase. These firing properties reflect geometric properties of the trajectory in phase space corresponding to the bursting solution. In fact, it is these geometric properties which uniquely characterize square-wave bursters and what distinguishes them from other classes of bursters.

We have already noted that bursting cannot arise in two-variable models. There is simply not enough room in a two-dimensional phase plane to generate the repetitive spiking. However, it is rather simple to generate bursting activity if we periodically drive a two-variable model. Consider, for example, the Morris-Lecar equations (4.1) with parameters given in Table 4.0.2 for the homoclinic regime. The bifurcation diagram, with bifurcation parameter I_{app}, is shown in Figure 6.2. The set of fixed points forms an S-shaped curve. There is a branch of periodic orbits which originates at a subcritical Hopf bifurcation along the upper branch of fixed points and terminates at an orbit homoclinic to the middle branch of fixed points.
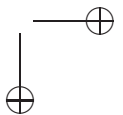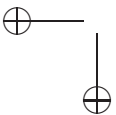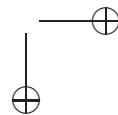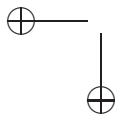
(The fact that the Hopf bifurcation is subcritical is not important here.) Moreover, there is an I_{app}-interval between $I_{app} = I_{HOM}$ and $I_{app} = I_{SN}$ for which the model is bistable: there are stable rest states along the lower branch of fixed points and stable, more depolarized, limit cycles. When $I_{app} = I_{HOM}$, there is a homoclinic orbit and when $I_{app} = I_{SN}$ there is a saddle-node bifurcation. Now suppose that I_{app} slowly varies back and forth across this interval. Because of the bistability, it is easy to see how a hysteresis loop is formed in which the membrane potential alternates between resting and spiking activity. Note that the frequency of firing slows down near the termination of the active phase. This is because the active phase ends as the solution crosses the homoclinic orbit.
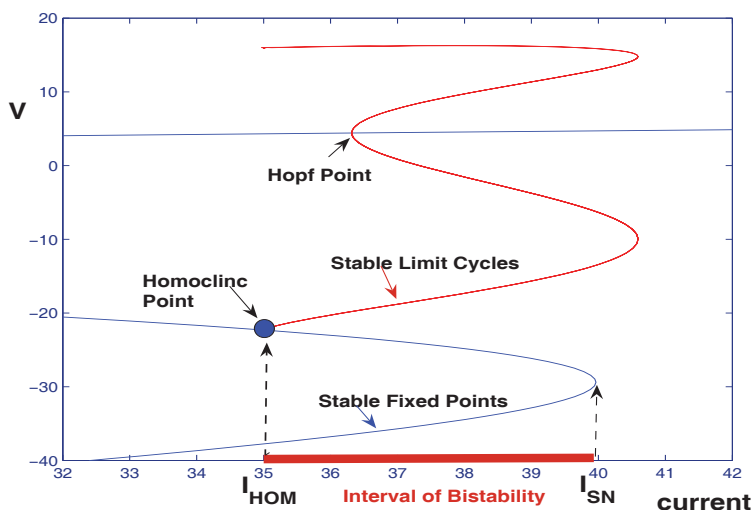
Figure 6.2. *A bifurcation diagram of the Morris-Lecar equations, homoclinic case. The set of fixed points form an S-shaped curve (not all of which is shown). A branch of limit cycles originates at a Hopf point and terminates at a homoclinic orbit. There is an interval of applied currents for which the system displays bistability.*

This example provides a simple mechanism, and geometric interpretation, for square-wave bursting. However, this mechanism is unsatisfactory since we imposed an external, periodic applied current. What we really wish to understand is autonomous bursting; that is, bursting that arises due to interactions among intrinsic properties of the cell. One way to achieve autonomous square-wave bursting is to again consider the Morris-Lecar model except now we redefine I to be a dynamic dependent variable that decreases during the active phase of repetitive firing and increases during the silent phase. This example demonstrates the basic principle that slow negative feedback together with hysteresis in the fast dynamics underlie square-wave bursting.

Many different ionic current mechanisms could produce the slow negative feed-

back. Here, we construct an autonomous model for square-wave bursting by starting with the Morris-Lecar model (4.1) and adding a calcium-dependent potassium current. The complete model can be written as:

$$C_m \frac{dV}{dt} = -g_L(V - E_L) - g_K n(V - E_K)$$
$$-g_{Ca} m_\infty(V)(V - E_{Ca}) - I_{KCa} + I_{app}$$

$$\frac{dn}{dt} = \phi(n_\infty(V) - n)/\tau_n(V)$$

$$\frac{d[Ca]}{dt} = \epsilon(\mu I_{Ca} - k_{Ca}[Ca]) \tag{6.2}$$

where the calcium-dependent potassium current I_{KCa} is given by

$$I_{KCa} = g_{KCa} z(V - V_K). \tag{6.3}$$

Here, g_{KCa} is the maximal conductance for this current and z is the gating variable with a Hill-like dependence on $[Ca]$, the near-membrane calcium concentration. Hence,

$$z = \frac{[Ca]^p}{[Ca]^p + 1}.$$

For simplicity, we set the Hill exponent $p = 1$. The third equation in (6.2) represents the balance equation for [Ca]. The parameter μ is for converting current into a concentration flux and involves the ratio of the cell's surface area to the calcium compartment's volume. The parameter k_{Ca} represents te calcium removal rate and ϵ is the ratio of free to total calcium in the cell. Since calcium is highly buffered, ϵ is small so that the calcium dynamics is slow. We shall refer to the first two equations in (6.2) as the fast-subsystem (FS) and the third equation as the *slow equation*.

Note that I_{KCa} is an outward current. If its conductance $g_{KCa}z$ is large, then the cell is hyperpolarized and the cell exhibits steady-state resting behavior. If, on the other hand, this conductance is small, then the cell can fire action potentials. Figure 6.3 shows the bifurcation diagram of (6.2), in which z is the bifurcation parameter. Note that the curve of fixed points is now Z-shaped, not S-shaped. There is a branch of limit-cycles that begins at a subcritical Hopf point and terminates at an orbit homoclinic to the middle-branch of fixed points. Finally, there is an interval of z-values for which the fast-subsystem exhibits both a stable fixed point and a stable limit cycle.

Now the full system exhibits square-wave bursting, as shown in Figure 6.1. Parameter values are given in Table 6.2. When the membrane is firing, intracellular calcium slowly accumulates, turning on the outward I_{KCa} current. When this current is sufficiently activated, the membrane can no longer maintain repetitive firing thus terminating the active phase. During the silent phase, intracellular calcium concentration decreases thereby closing KCa channels. Once enough outward channels are closed, the cell may resume firing.

The projection of the bursting solution onto the bifurcation diagram of the fast subsystem is shown in Figure 6.3B. During the silent phase, the solution trajectory
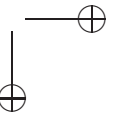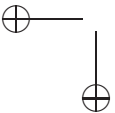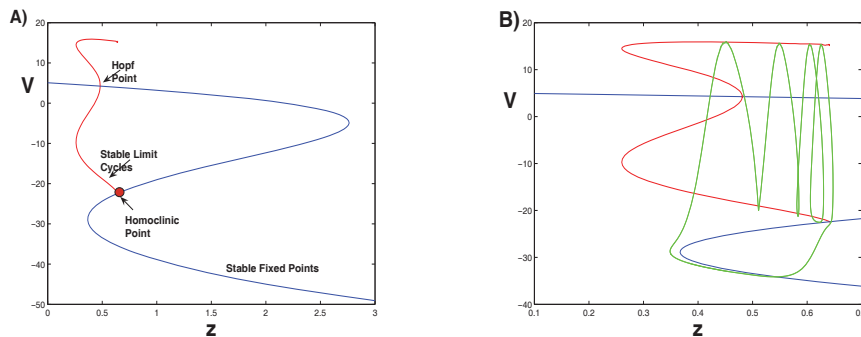
Figure 6.3. *(A) Bifurcation diagram of the fast-subsystem for square-wave burstering. (B) The projection of the bursting trajectory onto the bifurcation diagram.*

lies close to the lower branch of fixed points of the fast subsystem. The silent phase ends when the trajectory reaches the saddle-node of fixed points at which point the trajectory jumps close to the branch of stable limit cycles of the fast subsystem. While the membrane is spiking, the solution remains close to this branch until it crosses the homoclinic orbit of the fast-subsystem. The trajectory is then forced to jump down to the lower branch of fixed points and this completes one cycle of the bursting trajectory.

This example illustrates some of the basic features of square-wave bursting. We now consider a more general class of fast/slow systems and describe in more detail what geometric properties are needed to generate square-wave bursting. In general, square-wave bursting can arise in a system of the form (6.1) in which there are at least two fast variables and one slow variable. In order to obtain square-wave bursting, we must make assumptions on both the bifurcation structure of the fast subsystem and the slow dynamics. In order to describe these assumptions, we consider a three-variable model of the form:

$$
\begin{aligned}
v' &= f(v, w, y) \\
w' &= g(v, w, y) \\
y' &= \epsilon h(v, w, y, \lambda).
\end{aligned}
\tag{6.4}
$$

In the third equation, λ represents a fixed parameter. Later, we discuss complex bifurcations that arise when λ is varied. What distinguishes square-wave bursting is the bifurcation diagram of the fast subsystem: the set of fixed points of the fast subsystem forms a Z- (or possibly S-) shaped curve and there is a branch of stable limit cycles that terminate at a homoclinic orbit. The fixed points along the lower branch are stable with respect to the fast subsystem, while those fixed points along the middle branch are saddles with one stable and one unstable direction. The branch of limit cycles terminates at an orbit homoclinic to one of these saddles. In what follows, we denote the curve of fixed points of the fast subsystem as C_{FP} and